# MULTICOMPONENT DESIGN OF ROTOR-STATOR-NOZZLE (RSN) PROPULSOR ON AZIPODS

## MARINE 2017

## NIKOLAY V. MARINICH[*], ALEKSEY YU. YAKOVLEV[*], NIKOLAY A. OVCHINNIKOV[*] AND TOMI VEIKONHEIMO[†]

[*] Krylov State Research Centre
196158, St. Petersburg, Russia, 44, Moskovskoye shosse
e-mail: 10_otd@ksrc.ru, www.krylov-center.ru

[†] ABB Marine and Ports
P.O.Box 185, Merenkulkijankatu 1,FI-00981 Helsinki, Finland
e-mail: Tomi.Veikonheimo@fi.abb.com, www.abb.com/marine

**Key words:** Nozzled rotor, Post-swirl stator, Computational Methods, Design, Optimization, CFD calculation, Experiment

**Abstract.** The paper offers design computation method of RSN propulsor fitted with post-swirl stator on AZIPODs. The method implemented as problem solution of non-linear optimization of objective functional with restrictions over the field of infinitely dimensional values (functions being sought for). Numerical solution of this problem is reduced to the finite dimensional problem The shape of internal and external nozzle surface, distribution of pitch, camber, width and thickness of rotor blades and post-swirl stator geometry at radius are unknown functions of RSN propulsor design. Computational accuracy was validated through CFD-aided calculation of designed propulsors. Comparative analysis with model test results was implemented as well. The AZIPOD XL propulsor concept has been developed by the present method.

## 1 INTRODUCTION

Heavily loaded propellers are fitted with nozzles since the first half of the XXth century. In the extreme case - bollard pull, - mainly typical for tugs, nozzle allows doubling the propulsion thrust. Thrust increase at relatively low speed is also important for other kinds of ships, e.g. fishing, research, and support vessels. Tough positioning requirements for special-purpose vessels called into existence nozzled pods. Along with these propulsors, there also exist nozzled propellers for fast ships, see [1]. In a number of cases, nozzled propulsors have stator blades installed upstream or downstream of the propeller, see [1], [2].

Traditionally, nozzled propeller design is based on the diagrams of test series, see [3]. Later on, various methods of design calculation were used for propeller design, see [4], [5], [6], the nozzle shape normally remaining the same. These typical nozzle shapes are well known: D19*a* or more advanced ones, as per [7] and Soviet-developed OST nozzles [3].

Although there did appear a number of investigations on nozzle shape selection, e.g. [8], [9]. To some extent, integrated design of nozzled rotors was discussed in [10], [11], [12].

The approach to propulsor design must be holistic, so the potential of conventional design calculation methods cannot be used to the full. In this case, the methods based on direct numerical solution to the optimization problem are a universal tool. For nozzled rotors, this approach is used in [13].

## 2 PROBLEM STATEMENT

In view of the above, the purpose of this paper is to develop a design method for ducted rotor with post-swirl stator (RSN) (Fig. 1) as a totality of interwoven elements, that would yield better target parameters (efficiency, thrust) than those of conventional propulsor designs. This design method is based on direct optimization of propulsor components, and along with it, it should be fast and handy. The latter requirement determined the choice of BEM-methods with simplified consideration of viscous effects at the direct design stage and application of RANS-codes in further verification calculation.
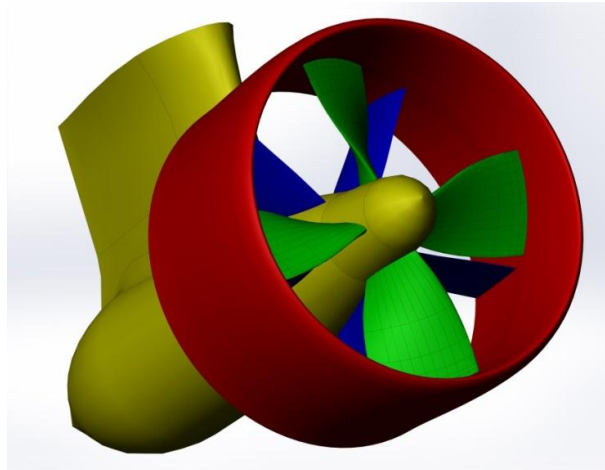


**Figure 1**: RSN propulsor (View of designed unite).

This design methods is based on the studies performed by Krylov State Research Centre, including vortex theory-based methods for verification of nozzled rotor calculations and Boundary Element Methods [14], design calculation method for nozzled propeller based on direct optimization, see [15] and [16], analysis of nozzle shape effect upon propulsor performance, see [9], [17] nozzle design method considering viscous effects, see [18]. All these studies made it possible to start the development of an integrated design method for nozzled rotors.

Nozzled rotors have a wide variety of applications, so it has to be determined what elements a nozzled propulsor will consist of and which of them require optimization. This paper discusses RSN propulsors with a single propeller, ring-shaped nozzle, axially symmetric hub and the stator blades downstream the propeller. The propulsor are mounted on the poded unite. All the components mentioned above are optimizable, however the pod shape was fixed.

## 3   METHOD OF NOZZLED PROPULSOR DESIGN

### 3.1  Propulsor design algorithm

The propulsor will be designed to the assumed power of the power plant. Once power, RPM and diameter are specified, it becomes possible to determine propeller torque coefficient $K_Q^*$ that will also be regarded as pre-defined. The mode of propulsor operation will depend on the propeller thrust and the force on post-swirl stator, so it may vary during design process.

The propulsor consists of several elements with completely different operation principles, so the design process is iterative, all the elements being designed one by one at each iteration stage. The fist calculation step is to desigh the propeller to the specified torque coefficient, the nozzle geometry being regarded as fixed. To optimize the propeller, it is necessary to specify inner advance ratio $J_S$ calculated for the flow rate Q at the nozzle in the section of the propeller disk.

$$J_S = \frac{4}{\pi} \frac{Q}{n D^3}$$

(1)

Here, n – rotation rate of rotor, D – rotor diameter.

To find this value, successive iterations are required because in the optimization to the specified torque coefficient, thrust coefficient $K_T$ that determines flow rate in the nozzle, only becomes known after the verification calculation is done. For each new propeller geometry, the stator is designed accordingly, and the optimal shape of nozzle is determined.

As nozzle optimization proceeds, the shape of the nozzle changes significantly, which has a strong effect upon the inner advance ratio. The nozzle also makes axial velocity distribution along the propeller disk radius non-uniform, which means the change in the operational conditions of the propeller, so one more iteration cycle is required. After several iterations, the process of propulsor optimization converges to the final solution.

### 3.2  Unified approach to optimization of specific propulsor components

As it was shown above, the algorithm mainly concerns optimization of specific propulsor elements. This optimization is based on a unified approach. Mathematically, determination of optimal shape for a body can be represented, in the most general form, as finding the minimum of a certain functional $I$, so as to satisfy a number of restrictions $G$, i.e.

$$\begin{cases} I(\varphi_j(x),...) \to \min \\ G_i(\varphi_j(x),...) \leq 0, i = \overline{1,n} \end{cases}$$

(2)

Here, $\varphi_j$ are target functions, and their number can be arbitrary.

Expressions for $I$ and $G_i$ may vary significantly, depending on the given task. At the same time, functions $\varphi_j$ involved in Expression (2) describe the shape of the body in the flow, so they must meet a number of requirements, including the requirements of continuity and piece-wise differentiability. On the other hand, $I$ and $G_i$ are usually found numerically, by means of boundary integral equation methods (BEM), and in future they could be obtained by means of RANS-methods, too. Accordingly, I and $G_i$ can be regarded as smooth, but not as differentiable.

Problem (2) is reduced to mathematical programming problem [19]. The problem of mathematical programming is formulated in the space of of $N$-dimensional vectors, where $N$ can be high but not infinite. Accordingly, the task is to discretize Problem (2), i.e. to pass from the real functions forming infinitely-dimensional space to the finite number of target parameters. This can be done by representing target function $\varphi_j$ as a linear combination of basis functions $f_k$.

$$\varphi_j(x) = \sum_{k=1}^{N_j} A_{kj} \cdot f_k(x) \tag{3}$$

Selection of basis functions depends on the specific task. From the narration above, it is clear that they must be continuous and have at least the first-order derivative continuous. The system of basis functions is generally selected so that they were orthogonal.

With expression (3) inserted into expression (2), optimization problem can be formulated as:

$$\begin{cases} \hat{I}(\vec{A}) \to \min \\ \hat{G}_i(\vec{A}) \le 0, i = \overline{1,n} \end{cases} \tag{4}$$

Here, $I$ represents the function of $n$-dimensional vector $A$ generated by target coefficients $A_{kj}$ in Expression (3), for all functions $\varphi_j$.

$$\vec{A} \in S \subset R^N, N = \sum_j N_j \tag{5}$$

Restrictions of problem $\hat{G}_i$ are also functions of $N$-dimensional vector $A$.

From the calculation viewpoint, Problem (4) is a non-linear problem of mathematical programming with restrictions, see [20]. In this case, the problem is solved by means of Powell method which is a variant of conjugate directions method. Its advantages are that is does not require calculation of derivatives and always converges to the local optimum, see [20].

Today, computers became significantly faster thanks to wide use of parallel calculations. But Powell method, as it is described in [20], is strictly sequential, so it had to be modified accordingly, see [19]. To see what efficiency parallel calculations could show in this case, test calculations were performed with various number of basis functions, and their results confirmed the efficiency of the algorithm based on parallel calculations, see [19].

## 3.3 Rotor optimization

Geometry of propeller blades is determined by several parameters being the functions of radius $r$ and distance measured along cylindrical cross-section chord $\xi$, see [3]. Blade width is selected so as to ensure necessary cavitation margin. The thickness is calculated as per the rules of the Classification Society selected. Distribution of blade pitch $P$ and camber $f$ over radius r are considered unknown, as well as blade area ratio $A_e/A_o$ of the rotor and maximum thickness $e(r)$ of its blades.

Objective functional in rotor optimization may be represented as:

$$I = 1 - \eta\left(P(r), f(r), \frac{A_e}{A_o}, e(r)\right) + k_1 \cdot \sqrt{\sigma(J^*)} + k_2 \cdot \sqrt{\sigma(J^* + \Delta J_1)} + k_3 \cdot \sqrt{\sigma(J^* - \Delta J_2)} \tag{6}$$

where $\eta$ is rotor efficiency, $\sigma$ – cavitation number, $J^*$ - advance ratio (i.e. ratio between ship speed $V$ and the pronozzle of rotation rate $n$ and rotor diameter $D$, $J = \dfrac{V}{nD}$) in design conditions, $\Delta J_1$, $\Delta J_2$ – desirable offset of cavitation bucket arms from the design advance, $k_1$, $k_2$, $k_3$ – coefficients ensuring the balance and simultaneously tending to increase efficiency and reduce the risk of cavitation.

Cavitation number $\sigma$ determines the pressure of cavitation inception on the blade. This number depends not only on the advance ratio but also on the rest of the target values:

$$\sigma = \sigma\left(J(r), P(r), f, \frac{A_e}{A_o}, E_{max}\right) \tag{7}$$

Selection of $k_i$ coefficients depends on the requirements the blade system has to meet.

The main restriction $G_1$ in this problem is that design torque coefficient $K_Q^*$ be equal to the specified one, $K_Q$.

$$G_1 = K_Q\left(P(r), f(r), \frac{A_e}{A_o}, E_{max}, J^*\right) - K_Q^* = 0 \tag{8}$$

Blade area ratio of the rotor is introduced in a standard manner [21] as a ratio between the area of the blades and the area of their circumscribed disk. In this case, the relationship between blade width and blade area ratio is linear. The requirement that this relationship remain linear is the second boundary condition:

$$G_2 = \frac{A_e}{A_o} - \frac{Z}{\pi R^2}\int_{r_h}^{R} C(r)\, dr = 0 \tag{9}$$

where $Z$ is blade number, $R$ – rotor radius, $r_h$ – hub radius.

To obtain an unambiguous solution, blade width distribution along radius $C(r)$ during optimization keeps its initial shape that must be defined in advance.

The change in the blade area ratio affect not only hydrodynamics of the rotor but its strength, too. To maintain the strength, an additional restriction was introduced, requiring to conserve the section modulus of the blade proportionate to the product of blade width and its square thickness, i.e.

$$G_3 = C(r) \cdot e(r)^2 = \Lambda_{rul}(r) \tag{10}$$

where $\Lambda_{rul}$ is selected so as to meet strength requirements of the Classification Society. Once this parameter is specified, it becomes possible to design a propulsor to the requirements of various Classification Societies for various classes of ships, depending on specific conditions:

During optimization, rotor parameters have to be recalculated many times, and this is performed as per the method described in [15] and being a variant of vortex method. This method yielded fairly good predictions of rotor parameters.

### 3.3 Stator optimization

Stator blade geometry is determined by the same parameters as the one of the rotor. Since stator not only improves thrust but also serves as a joint between the nozzle and the pod, width and thickness of stator blades must have sufficient strength margin. Unknown parameters are distributions of blade pitch $H$ and blade curvature $f$ along radius $r$.

Stator is the most efficient only when it fully utilizes the energy of the turbulent wake behind the rotor. Accordingly, the objective functional in rotor optimization must, apart from improving the parameters mentioned above, mitigate the energy of wake vorticity, i.e.

$$\int \left[ V_\theta(r) \right]^2 dr \to 0 \qquad (11)$$

where $V_\theta$ is tangential speed behind the stator.

In calculation of both stator and rotor parameters, the same method is applied, see [15], i.e. a variant of vortex method for fixed blades.

### 3.4 Nozzle optimization

Target functions in nozzle optimization are $r(x)$-type functions describing the shape of meridian nozzle section ($x$ – longitudinal coordinate, $r$ – nozzle radius), as well as inlet expansion ratio $\alpha$ (ratio between channel cross-sections at the nozzle inlet and in the propeller disk), outlet expansion ratio $\beta$ (ratio between channel cross-sections at the nozzle outlet and in the propeller disk) and relative nozzle extensions in certain cases.

For convenience of design, the surface of the nozzle can be split into three parts: external surface, internal surface upstream of propeller and internal surface downstream of propeller. Depending on operation conditions and purposes, it is possible to optimize both the entire surface of the nozzle and these parts severally. To optimize the external surface is to mitigate depressurizations and eliminate sharp pressure increases. The former condition improves cavitation performance of the nozzle, the latter one reduces the risk of boundary layer separation. To optimize internal nozzle surface upstream of propeller is to achieve constant pressure distribution throughout the nozzle surface. This optimization is sure to prevent cavitation and boundary layer separation upstream of the rotor. To optimize the area downstream of rotor is to achieve smooth pressure variation. All three parts of the nozzle are optimized simultaneously. In view of all these conditions, objective functional can be written as:

$$I = k_1 \cdot \int_{x_1}^{x_2} \left[ \frac{dCp}{dx} \right]^2 dx - k_2 \cdot \frac{2 \cdot T}{\rho \pi R^2 V^2} + \begin{cases} 0, & \dfrac{dCp_i}{dx_i} < 0 \\ k_3 \cdot \dfrac{dCp_i}{dx_i}, & \dfrac{dCp_i}{dx_i} > 0 \end{cases} \qquad (12)$$

where $C_P$ – pressure coefficient on the duct surfaces, $T$ – thrust of the unite, $k_1$, $k_2$ and $k_3$ are weight coefficients selected as per the given task.

Restricting conditions are as follows:
1) Specified flow rate must be preserved, i.e.

$$2\pi\int_{r_h}^{R} V_X \, r \, dr = Q^* \tag{13}$$

where $Q^*$ is specified flow rate in the nozzle, determined after calculation of propeller thrust and force at post-swirl stator, $V_x$ – velocity in propeller disc;

2)  The nozzle areas must be mated in a smooth manner, i.e.

$$r(x_1) = r^*(x_1), \quad \frac{dr}{dx}(x_1) = \frac{dr^*}{dx}(x_1)$$

$$r(x_2) = r^*(x_2), \quad \frac{dr}{dx}(x_2) = \frac{dr^*}{dx}(x_2) \tag{14}$$

where $x_1$ and $x_2$ – coordinates where the area to be optimized begins and ends; $r^*(x)$ – radius of the initial nozzle,

3) Flow separations must be eliminated (this condition shall be formulated as per the parameters of the boundary layer on the nozzle surface).

Calculation of the flow around the nozzle is performed as per the method described in [14], along with the calculation of the boundary layer on its surface and the assessment of flow separation risk, see [18].

## 4   DESIGN OF RSN PROPULSOR: CASE STUDY

Prior to optimization of nozzled rotor, it was investigated how the configuration of this propulsor affects its parameters. This investigation was necessary because nozzled propeller and RSN propulsor, although looking alike, have different hydrodynamic properties. In particular, the location of optimal efficiency of the RSN propulsor was found not to coincide with the efficiency optimum of known nozzled propeller series. Furthermore, special analytical and experimental assessment of the optimum location were performed for the RSN propulsor, with consideration of all its elements. The knowledge of the optimum point ultimately allows making RSN propulsor more efficient, light and compact.

After the main parameters of the propulsor under design were selected (see Table 1), the optimization was performed as per the procedure described above. The initial geometry of the rotor and the nozzle was the one applied in OST nozzles, see [3]. The rectifying apparatus had constant width and thickness distribution. Rotor and rectifying apparatus both had zero rake and skew of blades. The design included determination of optimal distribution for pitch and curvature of rotor and post-swirl stator along the radius, determination of nozzle shape, as well as its inlet and outlet expansion ratios. The objective of design was to maximize efficiency and achieve the best cavitation performance in design conditions. For the general view of designed propulsor, see Fig. 1.

As design proceeded, optimal shape was found for all the elements. In particular, final geometry of the nozzle eliminates depressurization zone at its front edge in design conditions and simultaneously ensures smooth pressure growth towards the rear edge (see Fig. 2), which prevents flow separation. Fig. 2 comparing pressure distributions along the internal and external surfaces of the designed nozzle and nozzle D19$a$ (if it is applied on this propulsor) clearly demonstrates optimization results. Reliability of the analytical assessments made in the design, was confirmed by CFD calculation results for the optimized geometry (see Fig. 2).

502

**Table 1:** Key parameters of RSN propulsor.

| Parameter | | Value |
|---|---|---|
| Operational conditions | Поступь $J$ | 1.065 |
| | Torque coefficient $K_Q^*$ | 0.065 |
| Rotor | Blade area ratio $A_e/A_o$ | 0.55 |
| | Blade number $Z$ | 4 |
| Nozzle | Relative elongation $l/D$ | 0.6 |
| | Location of rotor in the nozzle, $x_P/l$ | 0.4 |
| Stator | Blade number | 5 |



a)             b)
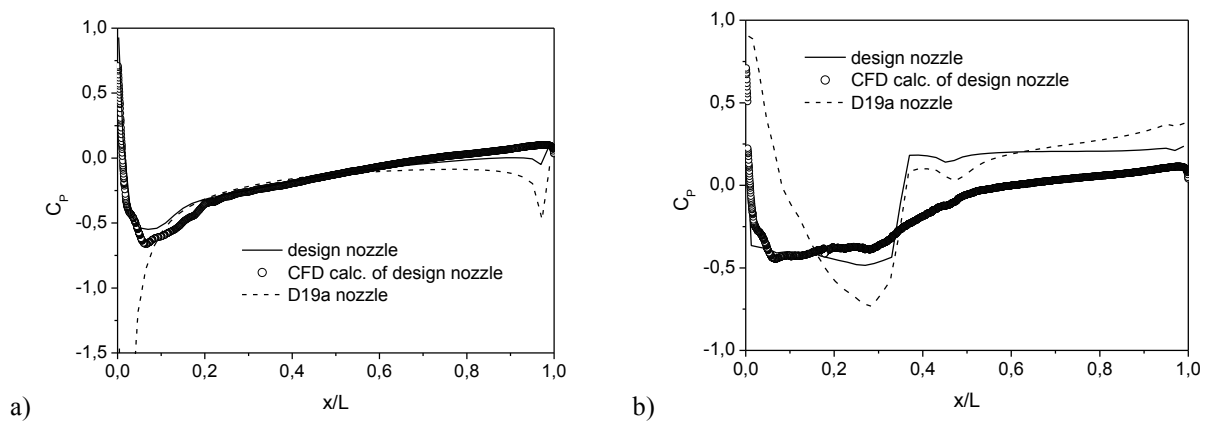
**Figure 2** : Distribution of pressure coefficient throughout the nozzle:
*a*) internal surface, *b*) external surface.

Distributed hydrodynamic parameters of the rotor were investigated in details as per the results of CFD calculation and are provided in Fig. 3 below. This Figure shows that pressure distribution throughout the rotor blade does not have any clear peaks, which confirms that the blades were designed correctly.



a)             b)
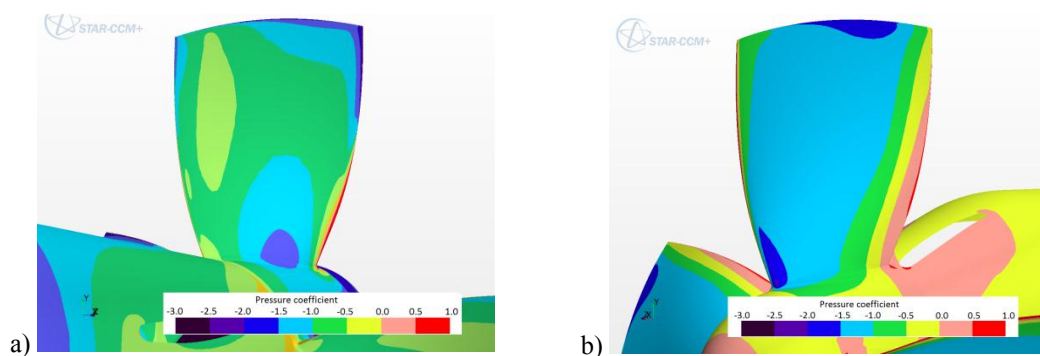
**Figure 3** : Pressures on the rotor blade as fractions of the maximum depressurization:
*a*) pressure side, *b*) suction side.

RSN propulsor design is an integrated process, i.e. all the elements of RSN propulsor have optimal parameters only if they operate jointly. Thus, according to the design calculation, the rotor-stator couple practically does not have any losses arising from wake vorticity. This is confirmed by CFD calculation data provided in Fig. 4. The Figure shows that although the vorticity downstream of the rotor is high and nonuniform, it is practically absent downstream of the stator.
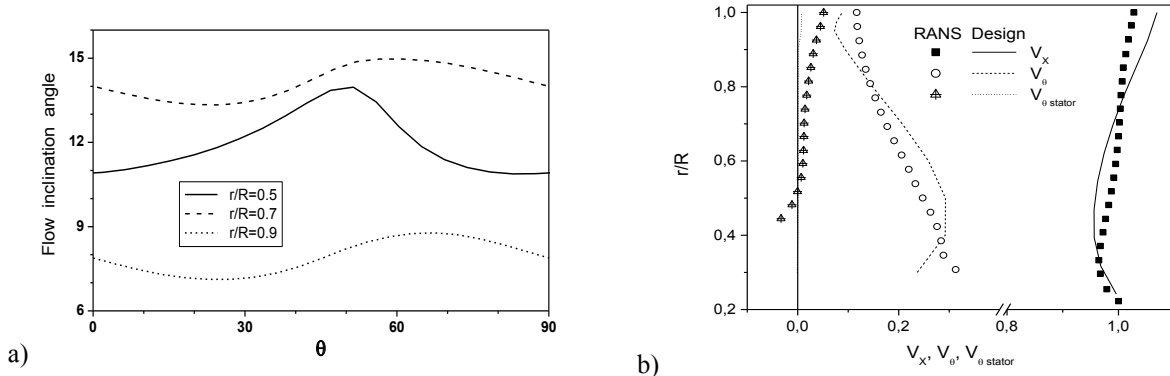


**Figure 4:** Speeds distribution a) tangential nonuniformity on a few radii before the stator, b) averaged speeds along radius before and after the stator.

Additionally, Fig. 5 shows the field of tangential speed $V_\theta$ at the nozzle outlet. Diagram (*a*) shows that tangential speed at the nozzle outlet in design conditions is practically zero. The non-uniformity in the upper segment occurs because of the overpressure generated by the strut. Along with it, diagram (b) shows that in non-design conditions tangential speed is non-zero all over the section. Accordingly, in the latter case the stator does not fully use the energy of turbulent wake behind the rotor. Comparison of these two diagrams clearly shows that the stator must be selected on case-to-case basis, for given operational conditions of the rotor. Any attempt to use a universal stator will hinder propulsor efficiency.
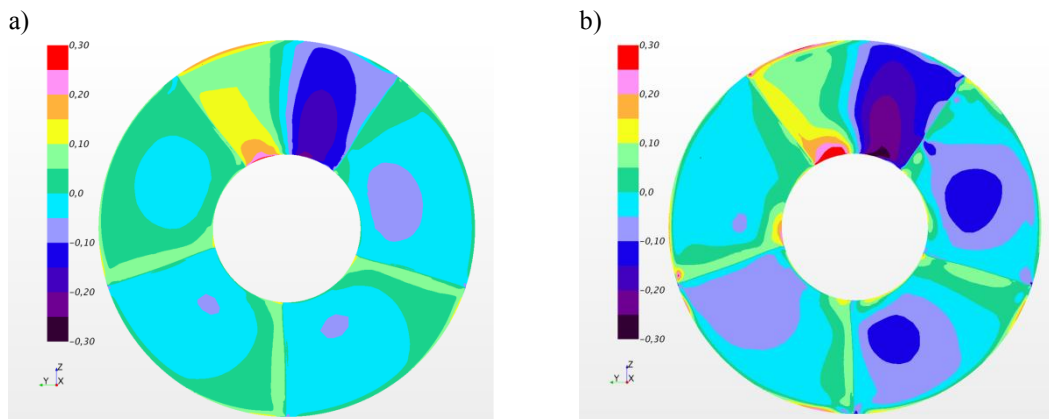


**Figure 5:** Tangential speeds at the nozzle outlet as fractions of the apparent speed of the propulsor movement: *a*) design conditions; *b*) non-design conditions ($J = 0.75 \cdot J^*$).

Force parameters of the propulsion system versus its advance ratio are shown in Fig. 6. The same Figure compares them with CD calculation results for the full-scale propulsor. Achieved efficiency of the propulsor was remarkably high, 69%, as per the data of the design calculation, i.e. in model test conditions. For the full-scale propulsor, CFD calculation yielded the efficiency of ~75%, and this difference is due to scale effect.
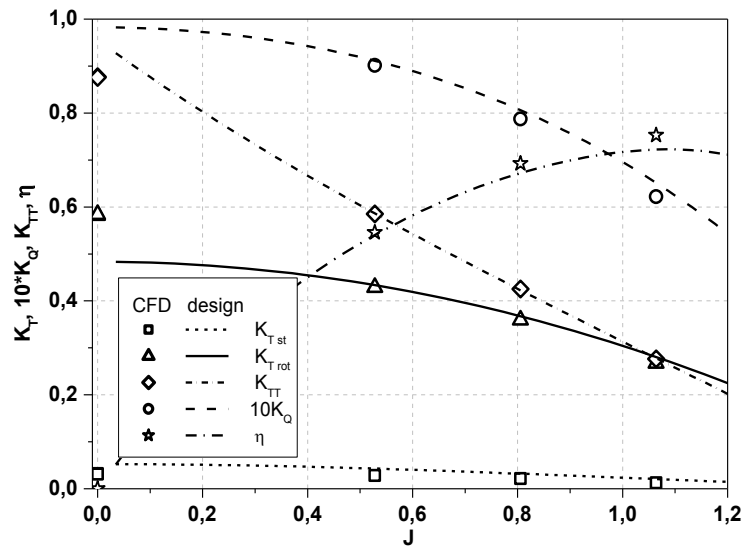


**Figure 6:** Performance curves of the designed propeller :
predictions (as per the results of the verification calculation) vs CFD calculation results.
Thrusts are shown as fractions of $\rho n^2 D^4$, torque is shown as fraction of $\rho n^2 D^5$.

Deviation between CFD calculation data and verification calculation results at bollard pull ($J$=0) is due to flow separation on stator blades. It occurs because the stator is designed to high-speed operation, so at bollard pull are at a large attack angle with respect to the flow. It is noteworthy that no flow separation will occur if the propulsor is designed specifically for bollard-pull operation. But in this case, the propulsor, albeit good at bollard pull, will not have required performance at full speed.

## 5  EXPERIMENTAL VALIDATION AND OPERATIONAL APPLICATIONS OF RSN PROPULSORS

This optimization method for RSN propulsors, successfully evaluated in the case study described above, was applied to develop propulsors of AZIPOD XL family to be installed on future ABB OY ships. This family includes various sizes of propulsors with different motor power. Unlike previous azimuthal thrusters with nozzled propellers, mainly intended to operate at low speeds, RSN propulsors of this family are meant to be main propulsors of commercial ships running at the speeds of over 20 knots. These propulsors have high full-scale efficiency, ~75%, as per preliminary estimates, including those confirmed by CFD calculations.

a)
b)
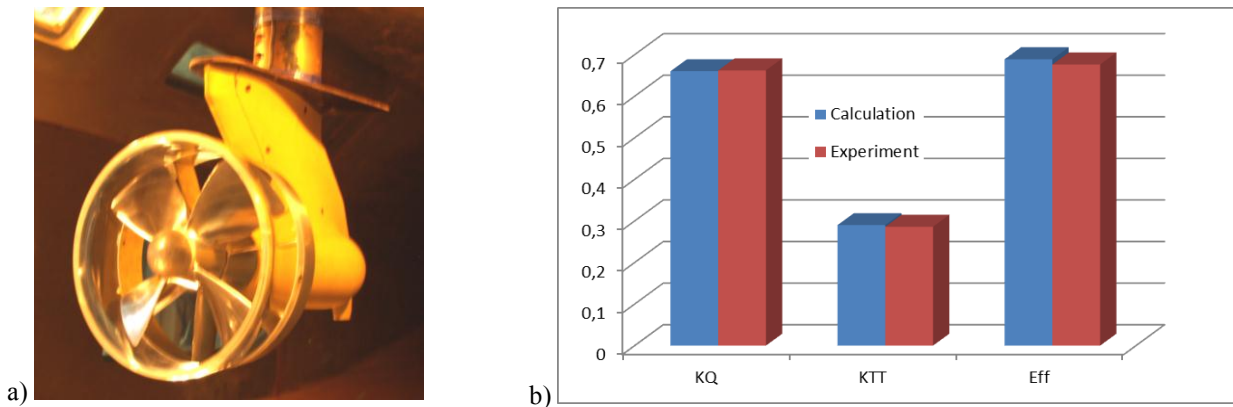
**Figure 7:** Model tests of RSN propulsors tests in KSRC:
*a*) cavitation testing; *b*) calculation data (*blue*) vs model test results (*red*).

The model tests of this propulsor family performed by KSRC confirmed accuracy and efficiency of the design calculations, as well as high performance of these propulsors. Fig. 7 compares design assessment of their performance parameters versus model test results..

## 6 CONCLUSIONS

- A design calculation method for RSN propulsor has been developed. This method is based on a set of analytical optimization techniques for all the elements of the propulsor, thus being considerably different from conventional methods of propulsor design;
- Optimization approach to design of RSN propulsors allowed identification their advantages, as well their utilization to the full. To achieve high parameters of RSN propulsor, the entire totality of its elements (rotor, stator, nozzle, etc.) must be optimized in an integrated manner;
- CFD calculations and model test data confirmed the efficiency of this method;
- This optimization method allowed the development of AZIPOD XL family of new highly efficient propulsors.

**REFERENCES**

[1] Van Blarcom, B., Franco Al, Lea, M., Peil, St., Dine, P. RIM-drive propulsion – improving reliability and maintainability over today's pods. *Proc. Of First international conference on technological advances in podded propulsion T-POD*. Newcastle, UK (2004).

[2] Wang, G. and Yang, Ch. Hydrodynamic performance prediction of ducted propeller with stators. *Journal of ship mechanics*. Vol. 3, No. 3, (1999) 1 – 7.

[3] Voytkunskiy, Ya.I. *Ship theory guide: In three volumes. Volume 1. Hydromechanics. Resistance to ship motion. Ship propulsors.* Leningrad, Sudostroenie (1985) (in russian).

[4] Mishkevich, V.G. *Development vortex theory methods as applied to design of sea-going vessel propulsors in order to reduce power requirements thereof.* Abstract of a thesis for Doctor of technical sciences, Leningrad (1986) (in russian).

[5] Stubblefield, J.M. *Numerically-based ducted propeller design using vortex lattice lifting line theory.* Massachusetts institute of technology, (2008).

[6] Gaggero, S., Rizzo, C. M., Tani, G., Viviani, M. EFD and CFD design and analysis of a propeller in decelerating duct. *International Journal of rotating machinery*. Article ID 823831, (2012).

[7] *SVA items*. No. 6 (2002).

[8] Dyne, G. An experimental verification of a design method for ducted propellers (Experimental validation of design method for ducted propeller). *Publ. of the Swedish State Shipbuilding experimental tank.* Nr.63, Goteborg (1968).

[9] Boushkovsky, V., Moukhina, L.,Yakovlev, A. Evaluation of duct shape influence on hydrodynamic and cavitational propeller characteristics. *ISC'2002 proceedings,* S.-Petersburg, Russia, (2002) 145-152.

[10] Kerwin, J. E. The preliminary design of advanced propulsors. *Proceedings Propellers/Shafting '03.* Virginia Beach, VA (2003).

[11] Nielsen, J. R. and Marinussen, H. Optimising propulsion systems for AHTS vessels. *Ship & Offshore.* № 2, (2010).

[12] Tamura, Y., Nanke, Y., Matsuura, M., Taketani, T., Kimura, K., Ishii, N. Development of a high performance ducted propeller. *ITS 2010.* Day 1, paper No. 7, Vancouver, Canada (2010).

[13] Huuva, T., and Pettersson, M. CFD optimizes nozzle design. *The Naval Architect. Marine propulsion supplement.* (2010) 19 – 22.

[14] Bushkovskiy, V. A. and Yakovlev, A. Yu. Boundary element method for streamlining prediction of bodies with axial symmetry. *Proceedings of the Krylov State Research Centre.* Issue 36(321), (2008) 187-200 (in russian).

[15] Vasiliev, A. V. and Yakovlev, A. Yu. Design method to assess hydrodynamic characteristics of axial pumps. *Abstracts of papers  XL Krylov readings* (2001) (in russian).

[16] Yakovlev, A. Yu. Design computation of blade systems through direct optimization methods. *Proceedings of the Krylov State Research Centre.* Issue 35(320), (2008) 111-121 (in russian).

[17] Moukhina, L. A. and Yakovlev, A. Yu. Optimization of components for propulsion system. *Proceedings of NSN-2007.* St. Petersburg, Russia, (2007) sA-23.

[18] Marinich, N.V. Optimization of duct shape. *Proceedings of the Krylov State Research Centre* (2012).

[19] Yakovlev, A. Yu. Parallel implementation of design methods for ship propulsor components. *Materials of VII international conference for computational mechanics and advanced applied software systems VMSPPS'2011.* Alushta. (2011) 265 – 267 (in russian).

[20] Minu, M. *Mathematical programming. Theory and algorithms.* "Nauka" (1990).

[21] Model manufacture, propeller models terminology and nomenclature for propeller geometry. *ITTC procedure 7.5-01-02-01.*